Ungrounded Lightning Surge Protection Device for Wireless Sensor Networks Node in the Wilderness

Qinghua Cao, Lixia Yang, and Shu Yan

School of Computer Science and Communication Engineering
Jiangsu University, Zhenjiang, 212013, China
cqh@ujs.edu.cn, lixiayang@yeah.net, yanshu@ujs.edu.cn

Abstract ─ In the wilderness, the use of wireless sensor network (WSN) nodes because of their maintenance-free remote-monitoring characteristic demands ungrounded lightning surge protection. This paper proposes a design of a protection device with functions of low-frequency surge cutting off and radio-frequency (RF) signal passing. In this device, the discharge circuit consists of a three-level surge by-pass circuit, an outer conductor antenna, and a copper-clad circuit board. The current capacity, start time, and output voltage meet the requirements of surge protection for a weak current device. Discrete components that provide the protective feature were involved in calculating impedance matching, and the parameters of these components were estimated and adjusted constantly at the test stage to ensure that the impedance of the inserted protection device matches with those of the node RF transceiver module and antenna. The experimental results show that the node with the ungrounded protection device can pass fourth-level surge immunity experiments and run for 49 months at the outdoor monitoring site in the Xinjiang coal fire area.

Index Terms ─ Impedance matching, lightning surge protection, ungrounded, wireless sensor networks.

I. INTRODUCTION

Lightning protection is an important topic of concern in the electromagnetic compatibility (EMC) research, and has a long history of developments made in heavy electricity-protection devices, with introduction of more mature technology [1–4]. In addition, many scholars have studied the different lightning characteristics [5−8]. With the development of large-scale integrated electronic systems, researchers began focusing on lightning protection related to weak electricity devices, and different protective devices and various application specifications were devised [9–12]. The WSN node deployed in the wilderness, with low voltage, low power, and high frequency, is a very special weak-electricity device, which requires a protection device with quick response, low output voltage, and large current capacity.

The communications and free-maintenance characteristics of the WSN node require that the protection device does not affect the transmission of signals and does not include a grounded device that must be maintained. To date, most existing protection devices are grounded [13], and some ungrounded protection circuits that have been devised have an applicable scope in the aspects of starting voltage, response speed, and current capacity [14]. In this study, the authors designed an ungrounded lightning protection device, which consists of a series circuit and three-level shunt circuit. The transfinite surge energy passed through the discharge circuit formed by a three-level discharge passage, copper-clad circuit board, and an outer conductor antenna, neutralizing the induced charge. The characteristic and import impedances matched with those of the antenna and radio-frequency (RF) transceiver module of a 2.4GHz WSN node. The minimum return loss, voltage standing wave ratio (VSWR) fit the requirements specified in the IEC Standard 62305-1 [11]. The results of a surge immunity test and field test show that an ungrounded protection device for the WSN node can defend against kilovolt/kilo-ampere lightning surges.

II. PERFORMANCE REQUIREMENTS

The lightning effects include direct and induction lightning, where the former shows strong damage ability and a small occurrence probability, whereas the latter shows a high occurrence probability and large impact scope [15]. According to the international standard of IEC 61000-4-5 [16], the time waveform of surge caused by induction lightning can be simulated using a combined wave of 1.2/50–8/20 μs, which increases to the withstand value of weak electricity device about several nanosecond. The frequency spectrum and energy concentration are in the low-frequency range of 0–100 kHz, and the peak is ranked in kV\kA.

The antenna of WSN nodes deployed in wilderness areas, when exposed to air, can receive signal and easily be at the risk of a lightning surge. Therefore, the protection device is mainly focused on the antenna feeder system.

A general WSN node is a low-voltage and low-current device, for example, the JN5139 node, with a working frequency of 2.4 GHz, working voltage of 2.2– 3.6 V, and withstand current of 150 mA. The surge waveform rises at the withstand voltage of the node for about a few milliseconds. Overall, the surge-protection circuit should have many technical indicators to meet the industry standards [12], such as response speed in nanoseconds, withstand voltage\current in kilovolts/kilo-ampere, an output clamping voltage between the node working voltage and maximum withstand voltage, a maximum continuous working voltage greater than 1.2 times the antenna feeder signal voltage, and a by-pass low-frequency surge. Impedance characteristics of the input and output ports should respectively match the impedance characteristics of the antenna and node, and the insertion loss and voltage standing wave ratio should meet the industry standards. All of these technical indicators are listed in Table 1.

Table 1: Technical indicators of surge protection device

Parameter	Requirement
Operating frequency	2.4 GHz
Current impulse withstand capability	kA
Voltage impulse withstanding capability	kV
Response time	ns
Transmission power	≥1.5×node power
Voltage standing wave ratio	≤1.2
Insertion loss	≥ −1 dB
Impedance characteristic	50 Ω

III. LIGHTNING SURGE PROTECTION CIRCUIT

The designed surge protection circuit for the antenna feeder system of WSN consists of a series circuit with a shunt part, as shown in Fig. 1.
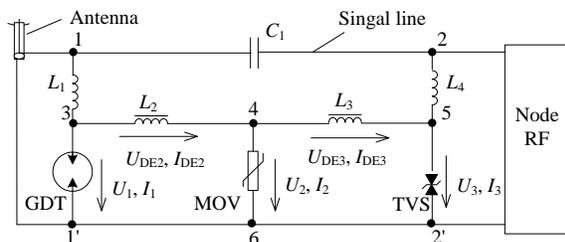

Fig. 1. Principle diagram of the antenna feeder surge protection circuit.

The series circuit comprises a signal line with capacitance C_1 placed between the antenna and node RF module, a cutoff low-frequency surge, and transit RF signal. Further, the shunt part comprises a discharge channel, and is composed of a gas discharge tube (GDT), metal-oxide varistor (MOV), and transient voltage suppressor (TVS). The output voltage, current capacity, and startup time of the three levels decline in turn. Based on these three channels, the signal line and outer conductor of the antenna form a discharge circuit. Inductances L_1 and L_4 separate the signal line from the surge discharge channel.

A. Operating principle of circuit

Under nomal conditions, the discharge channel closes. For th low-frequency surge wave, capacitor C_1 is equivalent to an open circuit and inductance L_1 is equivalent to a short circuit; thus, the voltage of port 1–1' is approximately equal to that of port 3–1'. When the surge approaches, the voltage at port 1–1', consisting of the work and surge voltages, rises quickly and takes approximately 3.5 ns to reach the node withstandable voltage. Then, the TVS with a small starting voltage and fast startup time, is the first to perform conduction, and the resulting output voltage is less than the tolerance voltage of the WSN node. The conduction path between ports 1–1' passes through 1–3–4–5–2'–1'. As the current of port 1–1' increases, inducted dynamic voltage U_{DE3} by inductance L_3 also increases. If the superposition value of U_{DE3} and TVS clamp voltage U_3 is greater than the open voltage of MOV, the secondary channel starts to discharge. In addition, if induced dynamic voltage U_{DE2} with the addition of MOV clamping voltage U_2 is greater than the starting voltage of GDT, the first main discharge channel discharges current to the copper-clad board and forms a loop with the outer conductor of the antenna line. As the clamp voltages of GDT, MOV, and TVS decrease progressively, the voltage difference between the stages is undertaken by inductances L_2 and L_3.

The three-level circuit requires coordinated work. The initial voltage, withstand current, and energy should abide by the following rules:

1) Before a subsequent level approaches the maximum tolerance energy, the following level starts functioning.

2) Before the following level is initiated, the subsequent level can withstand the surge current.

3) The startup voltage of the following level should be less than the withstand voltage of the subsequent level.

B. Determination of component types and parameters

According to the working principle of the protection circuit, coordination principle at all levels, and electrical characteristics of the node, the ESD5B5.0ST1G-type TVS, 20D180K-type MOV, and A81-C90X-type GDT [17–19] were selected.

1) Inductances L₂ and L₃

When the surge current increases rapidly, the induced electromotive force of the interstage inductance

pushes the first level of the protection component to start; this avoids excessive surge damage to the subsequent level. Figure 1 shows that the GDT discharge depends on whether the sum of U_2 and U_{DE2} is greater than GDT discharge voltage U_S:

$$U_1 = U_2 + U_{DE2} > U_S,\qquad(1)$$

where

$$U_{DE2} = L_2 \cdot \frac{dI_{DE2}}{dt}.\qquad(2)$$

From (1) and (2), the value of inductance L_2 can be derived as follows:

$$L_2 > \frac{U_S - U_2}{dI_{DE2}/dt}.\qquad(3)$$

For the 8/20-μs surge waveform with a 1-kA peak, $dI_{DE2}/dt \cong 0.1$ kA/μs. Further, $U_2 = 36$ V for the MOV clamp voltage [18], and GDT discharge voltage, $U_S = 600$ V [19]. When $L_2 > 5.64$ μH, the GDT can be pushed; therefore, inductance L_2 was set at 10 μH to leave some margin. By using the same method, the value of inductance L_3 that could push MOV to start was set at $L_3 > 1.08$ μH. To leave some margin, L_3 was set at 1.2 μH.

2) Capacitance C_1

In the RF band, inductances L_1 and L_4 segregate the signal line from the discharge channel, as shown in Fig. 1. In addition, capacitance C_1 and resistance R (50 Ω) of the WSN node constitute the RC high-pass filter. The voltage ratio between output and input is obtained as:

$$\dot{A} = \frac{R}{R + 1/j\omega C_1} = \frac{1}{1 + 1/j2\pi f RC_1},\qquad(4)$$

and the cutoff frequency is defined as:

$$f_L = 1/2\pi RC_1.\qquad(5)$$

To transmit the RF signal (2.4–2.4835 GHz), cutoff frequency f_L should be less than 2.4 GHz so that C_1 should be larger than 1.3 pF.

Table 2: Maximum transmission distance of the WSN node with a protection broad with different C_1

Capacitor Value (pF)	Transmission Distance (m)					
	Sunny, Empty Area	Sunny, 0.5 m Grass	Cloudy, Empty Area	Cloudy, 0.5 m Grass	Rainy Day, Empty Area	Rainy Day, 0.5 m Grass
1	200	120	208	95	190	83
3	240	135	220	105	196	88
5	272	142	225	103	198	89
10	233	117	193	94	175	84
15	220	103	186	90	169	82

Considering the influence of the distributed capacitance, inductance, and resistance in the RF circuit, the test method was used to determine the final value of C_1. As the transmission distance between two nodes can directly reflect the communication quality under the premise of no packet loss, the test method measures the maximum transmission distance with different C_1 values. Multiple test results under six conditions were averaged and are listed in Table 2. As shown, following a change in the capacitance value, the transmission distances are similar in all six environments. When C_1 increases from 1 to 5 pF, the transmission distance gradually increased, and then began to decrease when C_1 increased to 15 pF. Therefore, the final determination of C_1 is 5 pF.

C. Impedance matching

In this study, the discrete component of the protection device also undertakes impedance matching. For the RF signal, L_2 and L_3 are equivalent to an open circuit, and GDT and TVS have stray capacitance; thus, the protection circuit of Fig. 1 can be equivalent to Fig. 2.
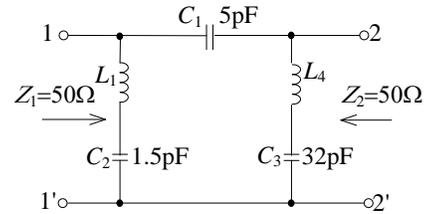

Fig. 2. Impedance-matching equivalent circuit of the protection circuit. Equivalent impedances Z_1 and Z_2 of port 1–1′ and 2–2′, respectively (Fig. 1).

In Fig. 2, C_2 and C_3 are the stray capacitances of GDT and TVS. Equivalent impedances Z_1 and Z_2 of ports 1–1′ and 2–2′, respectively, are equal to the characteristic impendences of the antenna and WSN node, and are defined as [20]:

$$Z_1 = \sqrt{Z_{oc1}Z_{sc1}},\qquad Z_2 = \sqrt{Z_{oc2}Z_{sc2}},\qquad(6)$$

where Z_{oc1} or Z_{sc1} is the equivalent impedance of port 1–1′ when port 2–2′ is an open- or a short-circuit; Z_{oc2} or Z_{sc2} is the equivalent impedance of port 2–2′ when port 1–1′ is an open- or a short-circuit:

$$Z_{oc1} = \left(j\omega L_1 + \frac{1}{j\omega C_2}\right) // \left(\frac{1}{j\omega C_1} + j\omega L_4 + \frac{1}{j\omega C_3}\right),\quad(7)$$

$$Z_{sc1} = \left(j\omega L_1 + \frac{1}{j\omega C_2}\right) // \left(\frac{1}{j\omega C_1}\right),\qquad(8)$$

$$Z_{oc2} = \left(j\omega L_4 + \frac{1}{j\omega C_3}\right) // \left(\frac{1}{j\omega C_1} + j\omega L_1 + \frac{1}{j\omega C_2}\right),\quad(9)$$

$$Z_{sc2} = \left(j\omega L_4 + \frac{1}{j\omega C_3}\right) // \left(\frac{1}{j\omega C_1}\right),\qquad(10)$$

where $Z_1 = 50$ Ω, $Z_2 = 50$ Ω, $C_1 = 5$ pF, $C_2 = 1.5$ pF [19], $C_3 = 32$ pF [17], and $\omega = 2\pi \times 2.4$ GHz. All of these parameters are substituted into (6)–(10) to compute L_4 and L_1 as follows: $L_4 \approx 5.4$ nH and $L_1 \approx 151$ nH. At this point, all discrete element models and parameters of the protection circuit have been established.

D. Ungrounded design

This device was designed for handling a low-grade lightning surge. The printed circuit board (PCB) of the protection device, excluding the signal lines and RF-signal channel area, is copper clad on both sides, which are connected via holes to an array to increase the volume. The thickness of the 140-μm copper foil is 4 times that of the ordinary PCB, thus improving the capacity of holding the electric charge as a buffer pool. The designed protection board is shown in Fig. 3.
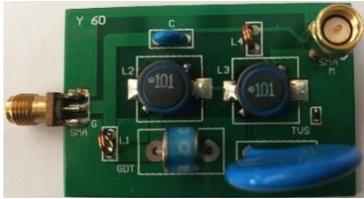

Fig. 3. The proposed surge-protection-device board.

IV. PERFORMANCE TEST

Based on the above-mentioned analysis, the ungrounded lightning surge-protection device was developed and tested according to the performance indicators in Table 1.

A. Return loss

Figure 4 shows the S_{11} curve of the surge-protection boards measured using a vector network analyzer.
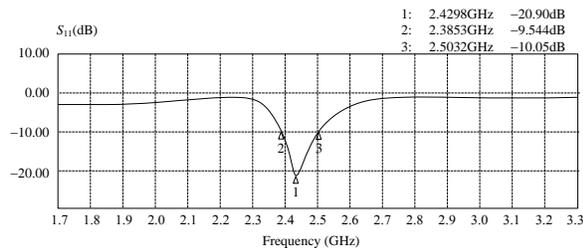

Fig. 4. S_{11} parameter curve of the surge protection device.

The center frequency in the frequency band of WSN node was 2.43 GHz; the minimum value of S_{11} was -20.9 dB, which approached the minimum value of the antenna. In addition, a -10-dB bandwidth (2.39–2.50 GHz) covers the frequency band of the WSN node (2.4–2.4835 GHz). According to the minimum S_{11}, the VSWR is calculated as 1.198.

B. (VSWR)

The relation of VSWR, S_{11} and reflection coefficient Γ is given as:

$$S_{11} = 20 \lg(\Gamma), \quad (11)$$

$$VSWR = \frac{(1+\Gamma)}{(1-\Gamma)}. \quad (12)$$

The minimum S_{11} value, as shown in Fig. 4, was substituted into (11) and reflection coefficient Γ at the center frequency point was obtained as 0.09, which was substituted into (12) to obtain VSWR of 1.198; this is less than the indicator value of VSWR in Table 1.

C. Insertion loss

Under the impedance-matching conditions of the port, the S_{21} parameter can represent insertion loss, and was measured using the vector network analyzer. Accordingly, the insertion loss at 2.43 GHz was obtained as -0.9 dB, which is greater than the value in Table 1.

D. Packet-loss probability test

The monitoring density of the WSN nodes that are deployed in reality is less than 100 m; therefore, the packet-loss probability was measured within this distance. Over a period of seven days, one node sent one data package per second. The number of packets received per hour was then counted and the average packet loss rate per hour was computed. The test result in Fig. 5 shows that the packet-loss probability does not show any obvious change before and after the addition of the surge protection device to the nodes.
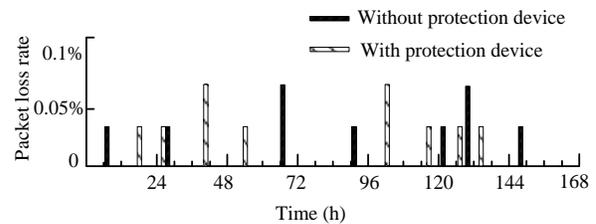

Fig. 5. Packet-loss rate of nodes with and without a surge-protection device.

E. Surge immunity test

The experimental conditions and test procedure were set as stipulated by the international standard of IEC 61000-4-5.

Experimental conditions: The test was conducted under standard climatic and electromagnetic environment conditions specified by the IEC 61000-4-5 standard. The environment temperature was 26 °C, relative humidity was 45%, and atmospheric pressure was 98 kPa. The lab environment was without electromagnetic interference.

Connection: As shown in Fig. 6, the antenna and another port of the protection device were separately connected through a combined-wave-signal generator and an RF port of the protected node. A 3.7V lithium iron phosphate battery was used to supply power to the node.

Testing program:

1) A four-level test was conducted with voltages from low to high: 0.5, 1, 2, and 4 kV.

2) The source impedance of the generator was 2 Ω.

3) The test surge wave numbers were calculated to obtain five each of positive and negative waveforms.

4) Repetitive rate: 1 time/min.

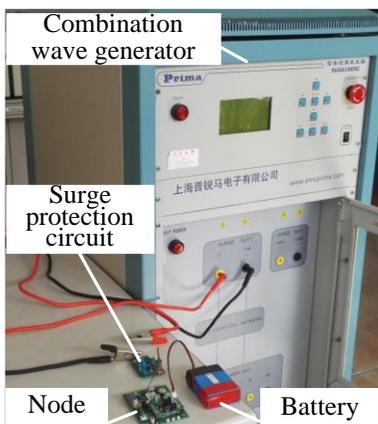According to the test plan, we conducted the tests many times, as shown in Table 3.

Fig. 6. Test connection diagram of the surge protection device.

Table 3: Experimental phenomena of surge immunity test

Test Level	Impulse Voltage (kV)	Surface Arc of GDT	Lines on PCB	Performance Character of Node	Peak Current of Node (mA)
1	0.5	Invisible	Intact	Normal	55
2	1	Visible	Intact	Normal	58
3	2	Clear	Intact	Normal	62
4	4	Bright	Intact	Normal	86

With the increase in test level, the GDT discharge intensity increased, and a dazzling arc gradually appeared on the GDT surface, indicating that a large amount of surge energy drains off through the GDT channel for protection. The line of the PCB is wider and thicker than that of a general board, and withstands the tests. During the testing, one node could continuously receive all the packets from another protected node, implying normal RF communication between the nodes. The performance characteristics, such as communication, distance, and packet loss, of the tested node are the same as those for an untested node. The peak current of the node increased with the increase in the test level, indicating that the surge affects the node's working current. After the surge test, the node's working current was measured again, and it was normal. Therefore, it can be concluded that the node with a protection device can pass the level-4 surge immunity test.

V. CONCLUSION

The protection circuit designed for WSN node bypasses the low-frequency surge and passes through the high-frequency signal. Protection components were installed at three levels of the bypass circuit and cooperated in start time and energy. When the bypass circuits are conducting successively, the RF signal line and outer conductor of the antenna form a closed loop through the TVS, MOV, and GDT. This loop can consume surge energy, and the thickness of the copper foil of the PCB can improve the capacity of holding the electric charge as a buffer pool. This helps the discharge circuit lines to withstand surge energy. The experimental results show that the node with the protection device can pass the standard level 4 of the surge immunity test. The proposed device was applied to the fire-monitoring network of the Xinjiang coalfield, and helped in the safe and continuous monitoring of the network for over four thunderstorm seasons. If we change the component types and parameters and adjust the working frequency and characteristic impedance, this ungrounded device could be used to protect other similar weak current devices.

ACKNOWLEDGMENT

REFERENCES

[1] M. A. Uman, *The Art and Science of Lightning Protection*. Cambridge University Press, Oxford, 2010.

[2] M. O. Goni and M. S. I. Hossaini, "Numerical electromagnetic analysis of GSM tower under the influence of lightning over-voltage," *ACES Journal*, vol. 24, no. 3, pp. 338-345, 2009.

[3] B. Glushakow, "Effective lightning protection for wind turbine generators," *IEEE Trans. Energy Convers.*, vol. 22, pp. 214-222, 2007.

[4] V.A. Rakov and F. Rachidi, "IEEE overview of recent progress in lightning research and lightning protection," *IEEE Trans. Electromagn. Compat.*, vol. 51, pp. 428-442, 2009.

[5] M. O. Goni and A. Ametani, "Analysis and estimation of surge impedance of tower," *ACES Journal*, vol. 24, no. 1, pp. 72-78, 2009.

[6] D. H. Trout, J. E. Stanley, and P. F. Wahid, "Evaluation of lightning induced effects in a graphite composite fairing structure," *ACES Journal*, vol. 26, no. 12, pp. 981-988, 2011.

[7] M. Izadi, M. A. Ab Kadir, and M. Hajikhani, "Evaluation of lightning current and ground reflection factor using measured electromagnetic field," *ACES Journal*, vol. 29, no. 1, pp. 107-115, 2014.

[8]   A. Karwowski, A. Noga, and T. Topa, "Computationally efficient technique for wide-band analysis of grid-like spatial shields for protection against LEMP effects," *ACES Journal*, vol. 32, no. 1, pp. 87-92, 2017.

[9]   P. Hasse, *Overvoltage Protection of low Voltage Systems*. 2nd ed., Institution of Electrical Engineers, United Kingdom, 2000.

[10] M. O. Goni, E. Kaneko, and H. Takahashi, "Thin wire representation of the vertical conductor in surge simulation," *ACES Journal*, vol. 19, no. 1, pp. 55-64, 2004.

[11] Protection against lightning - Part 1: General principles, *IEC Standard 62305-1*, 2010.

[12] Protection against lightning electromagnetic impulse - Part 3: Requirements of surge protective devices, *IEC Standard 61312-3*, 2000.

[13] S. Furukawa, A. Asakawa, and T. Hosokawa, "Experimental study on surge current to customer's facility owing to lightning stroke on television antenna," *2010 Asia-Pacific Symposium on Electromagnetic Compatibility*, Beijing, China, pp. 1181-1184, Apr. 2010.

[14] C. F. Barbosa and F. E. Nallin, "Lightning protection of a smart grid sensor,, *12th International Symposium on Lightning Protection*, Belo Horizonte, Brazil, pp. 273-277, Oct. 2013.

[15] V. Cooray, *Lightning Protection*. Institution of Engineering and Technology, London, 2009.

[16] Testing and measurement techniques – Surge immunity test, *IEC Standard 61000-4-5*, 2009.

[17] ON Semiconductor Inc., *ESD5B5.0ST1G datasheet*, Available: http://www.onsemi.com/pub/Collateral/ESD5B5.0ST1-D.PDF, 2017.

[18] World Products Inc., *20D180K datasheet*, June 8, 2011.

[19] EPCOS, *A81-C90X datasheet*, Available: https://en.tdk.eu/inf/100/ds/A81-C90X-X1380S102.pdf, 2015.

[20] D. M. Pozar, *Microwave Engineering*. Addison - Wesley Publishing Company, Boston, 1990.

Qinghua Cao received the B.S. degree in Information Engineering from Xi'an Jiangtong University, Xi'an, Shanxi, China, in 2000 and the M.S. degree in Communication and Information System from Lanzhou University, Lanzhou, Gansu, China, in 2004. She is currently pursuing the Ph.D. degree in Computer Application at Jiangsu University, Zhenjiang, Jiangsu, China. From July 2004 to now, she works at the School of Computer Science and Communication Engineering, Jiangsu University as a Lecturer. Her main research interest is in Wireless Sensor Networks.

Lixia Yang received the Ph.D. in Electronics Engineering from Xidian University, China, in 2007. He was a Postdoctoral Fellow of Electro Science Laboratory, Ohio State University, USA and worked at Space Science Laboratory, Dallas University, Dezhou, USA, as a Visiting Scholar. He is a Professor with the School of Computer Science and Communication Engineering, Jiangsu University, China, the Member of National Expert Committee of Electromagnetic Scattering and Backscattering, the Member of American Electromagnetic Research Institute, the Member of American Optical Society, the Senior Member of China Electronics Society. His research interests include electromagnetic scattering characteristics of complex targets (dielectric), antenna theory and design of communication system, RF microwave circuit design, time-domain computational electromagnetism.

Shu Yan received the B.S. degree in Physics, Nankai University, Tianjin, China, in 1978 and the Ph.D. degree from Department of Information and Communication Engineering of Xi'an Jiaotong University, Xi'an, Shanxi, China, in 2003. From October of 2005 to now, she works at the School of Computer Science and Communication Engineering, Jiangsu University, as a Professor, doctor adviser. Her research interests include Wireless Network, Computation Electromagnetics, Electromagnetic Field and Microwave Technology and Electric and Electromagnetic Exploration.